ACCSCIENCE PUBLISHING

Gene & Protein in Disease

ORIGINAL RESEARCH ARTICLE

Rational virtual screening, ADME, and molecular simulation studies of potential inhibitors of human superoxide dismutase 1 in a dysfunctional antioxidant system

Ayodele Sunday Alonge[1], Toluwase Hezekiah Fatoki[2]*, Iseoluwa Isaac Ajayi[1], Ibrahim Olabayode Saliu[3], Stanley Chukwuejim[4], Courage Dele Famusiwa[5], Oluwafijimi Adetuyi[4], and Ohunene Esther Joseph[1]

[1]Department of Biological Sciences, School of Life Science, Bamidele Olumilua University of Education, Science and Technology, Ikere, Ekiti State, Nigeria

[2]Applied Bioinformatics Laboratory, Department of Biochemistry, Faculty of Science, Federal University Oye Ekiti, Oye, Ekiti State, Nigeria

[3]Department of Genetics, School of Medicine, Washington University St. Louis, Missouri, United States of America

[4]Enzymology Laboratory, Department of Biochemistry, Faculty of Science, Federal University Oye Ekiti, Oye, Ekiti State, Nigeria

[5]Phytomedicine and Molecular Toxicology Research Laboratory, Department of Biochemistry, Faculty of Science, Federal University Oye Ekiti, Oye, Ekiti State, Nigeria

Abstract

Superoxide dismutase 1 (SOD1), a copper-dependent enzyme, facilitates the conversion of superoxide anions into hydrogen peroxide and oxygen, thereby regulating superoxide levels. Dysfunctions in SOD1 have been linked to neurodegenerative disorders such as amyotrophic lateral sclerosis, as well as liver and lung cancers. This study aimed to identify SOD1 modulators using *in silico* rational virtual enrichment screening, pharmacokinetics, docking, and molecular dynamic simulation (MDS). The findings yielded 38 compounds, predominantly exhibiting high gastrointestinal absorption but mostly non-permeable across the blood–brain barrier, with few exhibiting inhibitory effects on selected cytochrome P450s. Molecular docking revealed that compound 1 (PubChem CID: 36791369) exhibited the highest binding affinity (–6.771 kcal·mol^{-1}), followed by compound 19 (PubChem CID: 30935) with –6.468 kcal·mol^{-1}, and compound 20 (PubChem CID: 135744521) with –5.978 kcal·mol^{-1}. MDS and molecular mechanics/generalized Born surface area analysis indicated that the compound CID 36791369 – SOD1 complex and compound CID 30935 – SOD1 complex remained stable and energetically favorable under simulated physiological conditions at 0 ns and 100 ns. In conclusion, this study identified 38 compounds, among which compounds SN5, SN6, SN7, SN12, and SN25 emerged as potential inhibitors of SOD1 based on overall analyses. Further, research will be necessary to investigate the therapeutic effectiveness of these top five compounds *in vitro* and *in vivo* against SOD1.

Keywords: SOD1; Cancer; Amyotrophic lateral sclerosis; Novel inhibitors; Pharmacokinetics; Molecular docking; Molecular dynamics simulation

***Corresponding author:**
Toluwase Hezekiah Fatoki
(toluwase.fatoki@fuoye.edu.ng)

Citation: Alonge AS, Fatoki TH, Ajayi II, *et al.* Rational virtual screening, ADME, and molecular simulation studies of potential inhibitors of human superoxide dismutase 1 in a dysfunctional antioxidant system. *Gene Protein Dis.* 2024;3(2):3042.
doi: 10.36922/gpd.3042

Received: February 28, 2024

Accepted: April 18, 2024

Published Online: June 5, 2024

1. Introduction

The copper-dependent enzyme superoxide dismutase 1 (SOD1) belongs to the SOD enzyme family, which is distributed across various cell organelles.[1] SOD1 facilitates the conversion of superoxide anions into hydrogen peroxide and oxygen, thus maintaining low levels of superoxide. This function is crucial due to the toxicity and poor membrane permeability of superoxide.[1,2] SOD1, a copper/zinc-containing enzyme, is found in the cytosol, nucleus, and intermembrane space of mitochondria. In contrast, SOD2, a manganese-containing enzyme, resides in the mitochondrial matrix, and extracellular SOD (ecSOD or SOD3), a secreted copper-containing protein, is located in the extracellular matrix.[1,2]

Mutations in SOD1 are found in approximately 20% of amyotrophic lateral sclerosis (ALS)-affected families and can be inherited in autosomal dominant or recessive patterns.[3,4] Over 160 mutations in SOD1 have been linked to ALS, primarily comprising missense mutations along with a minority of small deletions and truncations.[5] Notably, misfolding and aggregation of mutant SOD1, rather than loss of enzymatic function, are central to ALS pathology.[6] Mutant SOD1 interacts with the dynein-dynactin complex in motor neurons, leading to impaired axonal transport and correlating with disease progression in SOD1 transgenic mice.[7,8]

In addition, SOD1 plays a crucial role in growth factor signaling in endothelial and tumor cells. SOD1-deficient mice have been demonstrated to exhibit increased susceptibility to liver tumors due to elevated DNA mutation rates.[9,10] Knockdown of SOD1 induces senescence in fibroblasts and decreases fertility in female mice.[11,12] Conversely, overexpression of SOD1 in lung cancer cells promotes growth by enhancing survival mechanisms, suggesting modulation of cellular redox status, including SOD1 inhibition, as a potential therapeutic strategy for cancer treatment.[13] In light of these considerations, this study aimed to identify potential SOD1 modulators using *in silico* rational virtual enrichment screening, pharmacokinetics, docking, and molecular dynamic simulations (MDSs).

2. Materials and methods

2.1. Protein-protein interaction (PPI) analysis

The 3D structure of the human SOD1 protein (UniProt ID: P00441, gene ID: SOD1), retrieved from the UniProt database (www.uniprot.org), served as the basis for this study. Its UniProt ID was subjected to PPI analysis using the STRING webserver (https://string-db.org/).[14]

2.2. Rational virtual screening

The UniProt ID of the protein was employed for rational enrichment virtual screening using the LIGQ webserver (www.ligq.qb.fcen.uba.ar), utilizing the full pipeline setting. LIGQ constructs a compound set with documented binding evidence to the input protein or similar ones, leveraging prior biological assays.

2.3. Clustering analysis

The obtained sets of ligands in SMILES format underwent scrutiny to eliminate any non-drug-like molecules. Subsequently, clustering analysis with multidimensional scaling was conducted on the ChemMine server (http://chemmine.ucr.edu/)[15] utilizing the ligands' SMILES representations.

2.4. *In silico* absorption, distribution, metabolism, and excretion (ADME) prediction

The compounds underwent *in silico* ADME screening using the SwissADME server (www.swissadme.ch),[16] employing default parameters and utilizing the SMILES format. Duplicated ligands and those with low gastrointestinal absorption (GIA) were subsequently excluded from further analyses.

2.5. Molecular docking

Molecular docking studies followed the protocol outlined by Fatoki *et al.*[17] Initially, the ligands' SMILES underwent 3D structure optimization using ACDLab/Chemsketch software and were saved in.mol format. Subsequently, PyMol software facilitated the conversion of ligand files from. mol to. pdb format. The 3D structure of human SOD1 was retrieved in AlphFold pdb format from the Uni Prot data base. Before docking, both the ligands and target protein structures in pdb format were converted to pdbqt format using AutoDock Tools v1.5.6.[18] Following this, ligand-protein molecular docking was performed utilizing AutoDock Vina v1.2.3.[19,20] Post-docking, binding affinity was determined, and close interactions between the ligands and targets were analyzed and visualized using ezLigPlot on the ezCADD web server available at http://dxulab.org/software.[21]

2.6. Molecular dynamics simulation

Molecular dynamics simulations were conducted for 100 ns using Desmond, a package of Schrödinger LLC.[22-24] The initial configurations of the protein and ligand complexes for molecular dynamics simulations were obtained from docking studies. Preprocessing of the protein-ligand complexes was performed using Maestro's protein preparation wizard, which included optimization and minimization of the complexes. All systems were prepared using the System Builder tool with the solvent model employing an orthorhombic box with TIP3P water molecules. The Optimized Potential for Liquid

Simulations 2005 (OPLS-2005) force field was utilized for the simulations, and the models were neutralized by adding 0.15 M NaCl counter ions to mimic physiological conditions.[25] The constant-temperature, constant-pressure (NPT) ensemble was selected with a temperature of 310 K and pressure of 1 atm for the complete simulation. Before the simulation, the models were relaxed. Trajectories were saved after every 100 ps during the simulation, and post-simulation analysis of the trajectories was conducted to determine root-mean-square deviation (RMSD), root-mean-square fluctuation (RMSF), and protein-ligand interaction profiles. In addition, prime molecular mechanics/generalized Born surface area (MMGBSA) calculations were performed to evaluate the binding free energy (ΔG^{bind}) of the complexes,[23,24,26] as shown in Equation I:

$$\text{MMGBSA } \Delta G^{bind} = \Delta G^{Coulomb} + \Delta G^{Covalent} + \Delta G^{Hbond} + \Delta G^{Lipo} + \Delta G^{Packing} + \Delta G^{SolvGB} + \Delta G^{vdW} \quad \text{(I)}$$

3. Results

In this study, the PPI analysis of human SOD1 predicted its primary interacting proteins, including SOD2, CCS (copper chaperone for SOD), BCL2 (apoptosis regulator Bcl-2), PARK7 (Parkinson's protein 7 or protein/nucleic acid deglycase DJ-1), VDAC (voltage-dependent anion-selective channel protein 1), FUS (RNA-binding protein FUS), TARDBP (TAR DNA-binding protein 43), NEFL (neurofilament light polypeptide), HSPA5 (endoplasmic reticulum chaperone BiP), and DERL1 (Derlin-1), as depicted in Figure 1.

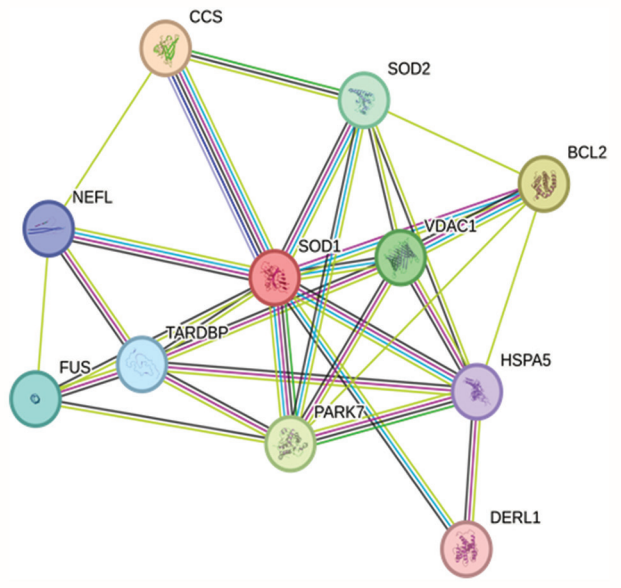

Figure 1. Protein-protein interaction profile of superoxide dismutase 1

Enrichment virtual screening was conducted on human SOD1 to identify compounds with potential modulatory effects. The virtual screening yielded 72 compounds in SMILES format (Supplementary File S1). Hierarchical clustering of these compounds revealed their structural similarities, as illustrated in Figure 2. In addition, pharmacokinetic prediction was performed on the 72 compounds, with results presented in Supplementary File S2. Following manual inspection of the pharmacokinetic results, duplicated compounds and those with low GIA were excluded from the study. This process yielded 38 chemical

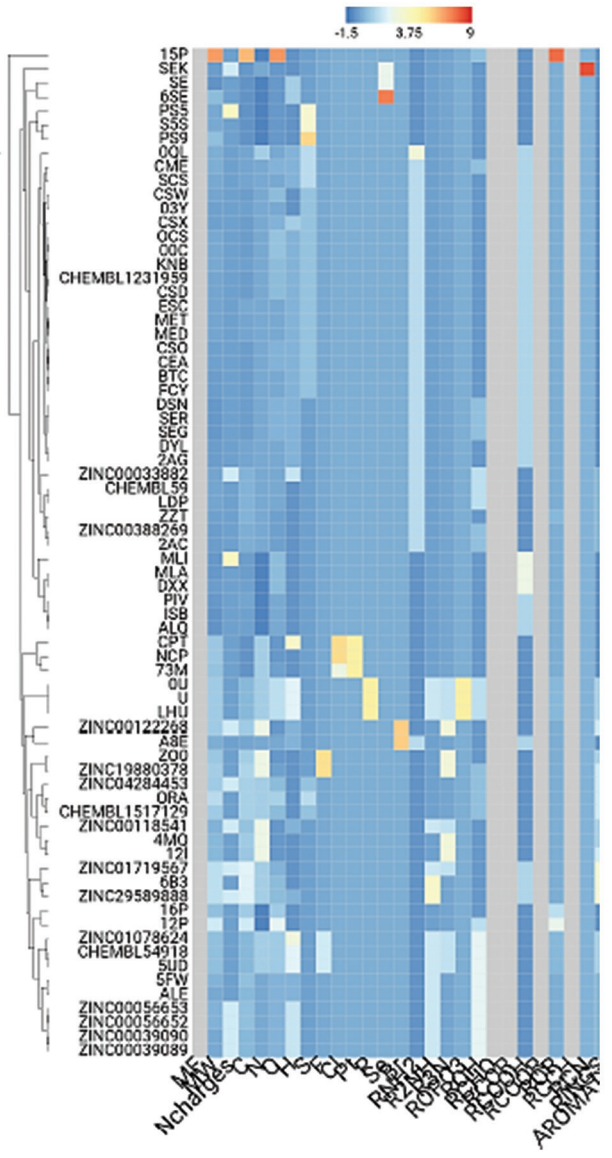

Figure 2. Hierarchical clustering results. Parameter options used are Heatmap (distance matrix), Linkage Method (single), Physicochemical Properties Heatmap (ChemmineR Properties), and Properties Color and Display Values (Z-scores).

compounds with high GIA, predominantly impermeable to the blood-brain barrier (BBB), possessing good solubility, and exhibiting minimal inhibitory effects on selected cytochrome P450s, as summarized in Table 1.

The SMILES of the 38 compounds were cross-checked on the PubChem database, and their corresponding PubChem CIDs were obtained. Subsequently, molecular docking analyses were conducted on these compounds. The results of the molecular docking revealed the binding affinities of human SOD1 for 38 analyzable compounds, as presented in Table 2. Compound 1 (PubChem CID: 36791369) exhibited the highest binding affinity of -6.771 kcal·mol^{-1}, followed by compound 19 (PubChem CID: 30935) with -6.468 kcal·mol^{-1}, compound 20 (PubChem CID: 135744521) with -5.978 kcal·mol^{-1}, and others. The IUPAC names of the top three compounds are 2-[2-[(6-oxo-5H-phenanthridin-3-yl) carbamoyl]phenyl]benzoate, 3-[(2-hydroxynaphthalen-1-yl) diazenyl]benzenesulfonic acid, and 3-[(2-hydroxynaphthalen-1-yl)diazenyl]benzenesulfonate, respectively. The binding poses of the complexes with high binding affinities are depicted in Figure 3, illustrating the involvement of specific

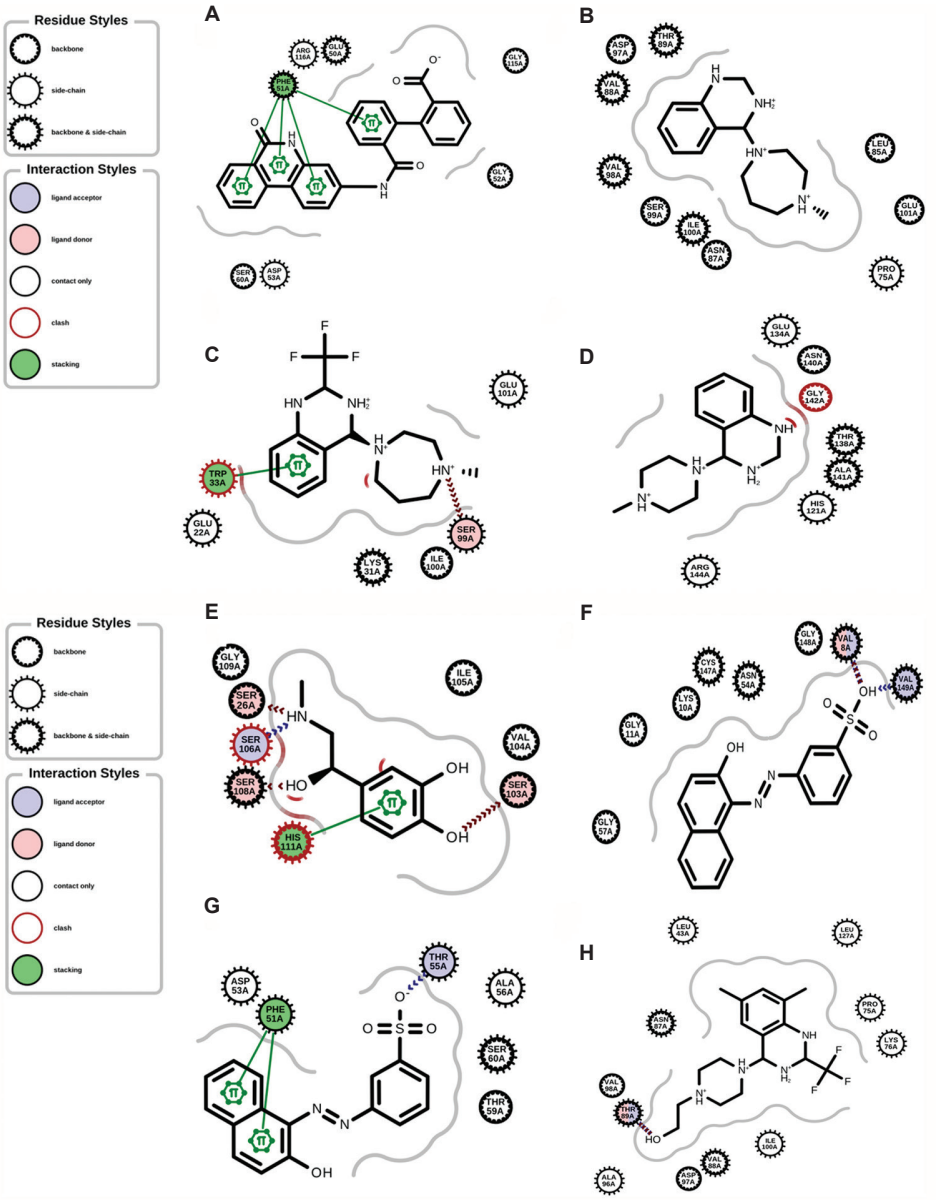

Figure 3. Interaction of the binding poses of soluble epoxide hydrolase with (A) PubChem CID: 36791369, (B) PubChem CID: 47121004, (C) PubChem CID: 17445796, (D) PubChem CID: 21029584, (E) PubChem CID: 5816, (F) PubChem CID: 30935, (G) PubChem CID: 135744521, and (H) PubChem CID: 993363.

Table 1. Predicted pharmacokinetics of 38 compounds with high low gastrointestinal absorption GIA

S. No.	Ligands code	Predicted ADME parameter from SWISSADME												
		MW	MR	TPSA (Å²)	Log P	ESOL Log S	ESOL class	GIA	BBB	P-gp	CYPs	Lip	BS	SA
1	ZINC29589888	433.43	126.74	102.09	4.02	−5.58	Moderately soluble	High	No	No	2C9, 2C19	0	0.56	2.76
2	ZINC00388269	123.15	37.84	46.25	1.18	−1.83	Very soluble	High	Yes	No	3A4	0	0.55	1
3	CHEMBL1231959	152.15	28.92	129.55	−2.9	1.73	Highly soluble	High	No	No	-	0	0.55	2.28
4	KNB	167.18	34.79	105.84	−1.94	1.84	Highly soluble	High	No	No	-	0	0.55	2.61
5	4MQ	242.32	80.61	32.26	1.89	−3.1	Soluble	High	Yes	Yes	1A2, 2D6	0	0.55	2.24
6	ZO0	310.32	85.61	32.26	2.99	−3.92	Soluble	High	Yes	Yes	1A2, 2C19, 2D6	0	0.55	2.5
7	12I	228.29	75.8	32.26	1.64	−2.82	Soluble	High	Yes	Yes	1A2	0	0.55	2.03
8	ZINC00056653	212.27	59.9	77.3	−0.89	1.01	Highly soluble	High	No	No	-	0	0.55	2.08
9	MET	149.21	38.22	88.62	−0.59	0.68	Highly soluble	High	No	No	-	0	0.55	2.43
10	ESC	163.24	43.03	88.62	−0.23	0.42	Highly soluble	High	No	No	-	0	0.55	2.66
11	ZINC00039090	184.21	50.29	77.3	−0.81	−0.26	Very soluble	High	No	No	-	0	0.55	1.82
12	ALE	183.2	49.03	72.72	0.1	−0.26	Very soluble	High	No	No	-	0	0.55	1.79
13	PS5	160.32	37.5	75.9	0.1	−0.26	Very soluble	High	No	No	-	0	0.55	1.79
14	S5S	163.35	42.14	167	0.1	−0.26	Very soluble	High	No	No	-	0	0.55	1.79
15	PS9	256.52	60.73	202.4	0.1	−0.26	Very soluble	High	No	No	-	0	0.55	1.79
16	CSO	137.16	30.18	108.85	−1.82	1.78	Highly soluble	High	No	No	-	0	0.55	2.45
17	CSD	153.16	30.86	119.83	−2.2	2.05	Highly soluble	High	No	No	-	0	0.56	3.05
18	PIV	102.13	27.66	37.3	0.99	−1.33	Very soluble	High	Yes	No	-	0	0.85	1
19	CHEMBL1517129	328.34	86.45	107.7	3.09	−4.3	Moderately soluble	High	No	No	-	0	0.56	3.01
20	ZINC04284453	327.33	84.6	110.53	3.02	−4.29	Moderately soluble	High	No	No	2C19	0	0.56	2.98
21	16P	294.38	75.92	55.38	1.62	−0.51	Very soluble	High	Yes	No	-	0	0.55	3.15
22	SER	105.09	22.18	83.55	−1.97	1.57	Highly soluble	High	No	No	-	0	0.55	1.51
23	OCS	169.16	31.55	126.07	−2.43	2.13	Highly soluble	High	No	No	-	0	0.56	2.82
24	CSW	153.16	30.86	119.83	−2.24	2.05	Highly soluble	High	No	No	-	0	0.56	3.05
25	ZINC19880378	354.37	96.7	52.49	2.83	−3.81	Soluble	High	Yes	Yes	1A2, 2D6	0	0.55	2.66
26	CHEMBL59	153.18	42.97	66.48	0.46	−0.44	Very soluble	High	No	No	-	0	0.55	1.01
27	ZINC00033882	154.19	44.23	68.1	−0.42	−0.45	Very soluble	High	No	No	-	0	0.55	1.04
28	MLA	104.06	20.08	74.6	−0.65	0.16	Highly soluble	High	No	No	-	0	0.85	1
29	DXX	118.09	24.89	74.6	−0.23	−0.48	Very soluble	High	No	No	-	0	0.85	1.08
30	CME	197.28	46.97	134.15	−0.99	0.7	Highly soluble	High	No	No	-	0	0.55	3.09
31	SCS	181.28	45.81	113.92	−0.27	0.07	Highly soluble	High	No	No	-	0	0.55	2.97
32	FCY	121.16	28.94	102.12	−1.31	1.11	Highly soluble	High	No	No	-	0	0.55	1.75
33	03Y	135.18	33.79	102.12	−1.12	1.27	Highly soluble	High	No	No	-	0	0.55	1.84
34	6SE	238.9	19.49	0	−1.12	1.27	Highly soluble	High	No	No	-	0	0.55	1.84
35	ZINC00118541	217.29	67.42	42.25	0.81	−2.93	Soluble	High	No	No	-	0	0.55	2.01
36	ZINC00122268	322.22	89.27	33.46	1.55	−3.9	Soluble	High	No	Yes	1A2	0	0.55	2.31
37	A8E	194.03	38.02	63.32	−0.34	0.28	Highly soluble	High	No	No	-	0	0.55	2.64
38	DYL	115.13	30.15	63.32	−0.83	1.07	Highly soluble	High	No	No	-	0	0.55	1.87

Notes: Physicochemical properties: Molecular weight (MW), molar refractivity (MR), total polar surface area (TPSA). Lipophilicity: Consensus Log P. Water Solubility: ESOL Log S, ESOL Class. Pharmacokinetics: gastrointestinal absorption (GIA), blood-brain barrier (BBB), P-glycoprotein (P-gp) substrate, inhibition of cytochrome P450 (CYPs) type CYP1A2, CYP2C19, CYP2C9, CYP2D6, and CYP3A4. Druglikeness: Lipinski (Lip), bioavailability score (BS). Medicinal chemistry: synthetic accessibility (SA).

Table 2. Molecular docking results

S. No.	Phytochemicals	PubChem CID	SOD1 (Alpha-Fold ID: AF-P00441) binding affinity ΔG (kcal·mol^{-1})
1	ZINC29589888	36791369	−6.771*
2	ZINC00388269	7264	−4.106
3	CHEMBL1231959	6398956	−4.136
4	KNB	11283261	−3.991
5	4MQ	47121004	−5.796*
6	ZO0	17445796	−5.739*
7	12I	21029584	−5.549*
8	ZINC00056653	6921600	−4.952
9	MET	6137	−3.966
10	ESC	25674	−3.895
11	ZINC00039090	6920144	−4.781
12	ALE	5816	−5.057*
13	PS5	5289210	−2.104
14	S5S	NA	−1.935
15	PS9	66348	−2.459
16	CSO	165339	−3.569
17	CSD	1549098	−4.164
18	PIV	6417	−3.507
19	CHEMBL1517129	30935	−6.468*
20	ZINC04284453	135744521	−5.978*
21	16P	90206	−3.058
22	SER	5951	−3.927
23	OCS	72886	−3.979
24	CSW	109	−4.008
25	ZINC19880378	993363	−5.756*
26	CHEMBL59	681	−4.923
27	ZINC00033882	3713609	−4.255
28	MLA	867	−3.818
29	DXX	487	−4.022
30	CME	170018	−4.239
31	SCS	480046	−3.937
32	FCY	5862	−3.529
33	03Y	9989321	−3.695
34	6SE	137348516	−1.49
35	ZINC00118541	5078469	−4.663
36	ZINC00122268	3449846	−5.053*
37	A8E	2762282	−3.938
38	DYL	14044	−3.845

Notes: NA: Not available. Docking parameter: SOD1 (spacing: 0.375, NTPS: 106×106×106, center: 1.984×2.466×3.811). *Suitable score.

amino acid residues in the binding interactions. SOD1 amino acid residues PHE51, TRP33, and HIS111 participate in pi-stacking interactions, while SER99, SER103, SER26, and SER108 act as the main ligand hydrogen donors. In addition, THR55 and VAL149 serve as the primary ligand hydrogen acceptors.

MDSs were conducted to evaluate the structural stability of both the protein and the binding status of the ligand in a physiologically relevant environment. The binding complexes of human SOD1 with the two compounds exhibiting the best binding affinities (PubChem CID 36791369 and PubChem CID 30935) were utilized for MDS analysis to facilitate comparison. The outcomes of these MDS analyses are depicted in Figure 4A-F, providing valuable insights into the dynamic behavior and interactions of the protein-ligand complexes under realistic conditions.

The binding complex of SOD1 with compound CID 36791369 exhibited an RMSD of the protein ranging from 0 to 100 ns, with a value of 2.25 Å. Conversely, for the ligand, the RMSD was 19 Å during the same period (Figure 4A). The RMSF analysis of SOD1 revealed maximal fluctuations at amino acid residues 50 – 55 and 125 – 135 (Figure 4B). Protein-ligand interactions included hydrophobic interactions, hydrogen bonds, and water bridges involving amino acid residues such as HIS49, THR59, HIS64, GLY142, and ARG144 (Figure 4C). Similarly, for the binding complex of SOD1 with compound CID 30935, the RMSD of the protein was 2.25 Å, and that of the ligand was 15 Å from 0 to 100 ns (Figure 4D). The RMSF showed maximum fluctuation at amino acid residues 125 – 135 (Figure 4E). The protein-ligand interactions comprised hydrophobic interactions, hydrogen bonds, water bridges, and ionic interactions involving amino acid residues such as VAL8, LYS10, ASN54, and CYS147 (Figure 4F).

The results of MDS demonstrated suitable stability and interactions between compound CID 36791369 and SOD1, with major amino acid residues including HIS49, HIS64, HIS121, GLY142, and ARG144. Similarly, compound CID 30935 exhibited interactions with SOD1 involving LYS10, ASN54, and CYS147 as major amino acid residues. A schematic detailing the interactions between the ligand atoms and protein residues is presented in Figure 5. Overall, the protein-ligand interaction profiles validated the amino acid residues identified in the docking interactions. The binding free energies for all complexes were computed using MMGBSA at both 0 and 100 ns time points. The MMGBSA results (Table 3) revealed a binding energy ΔGbind (Total) of -32.867 and -56.110 kcal·mol^{-1} for the compound CID 36791369 – SOD1 complex at 0 ns and 100 ns, respectively. For the compound CID 30935 – SOD1 complex, the values were -28.518 and -39.790 kcal·mol^{-1} at 0 ns and 100 ns, respectively. These calculations indicate

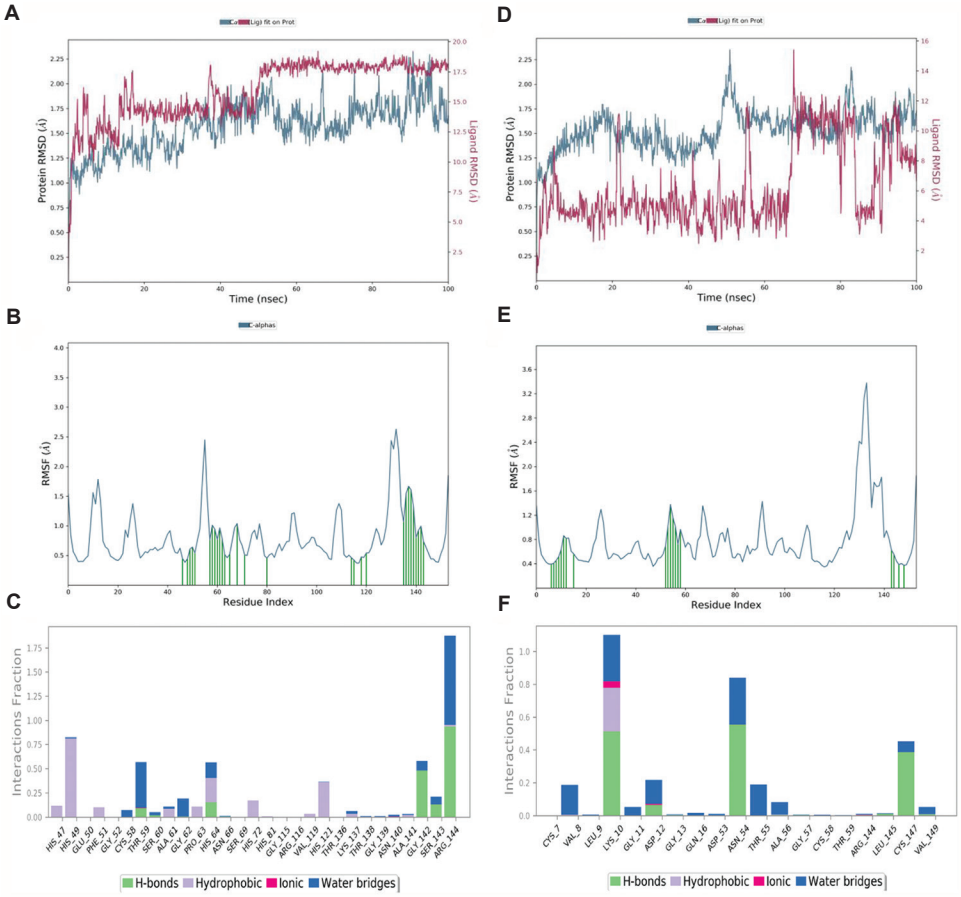

Figure 4. Protein-ligand complex simulation results. (A) RMSD of compound CID 36791369 – SOD1. (B) RMSF of SOD1. (C) Interaction profile of the contact between compound CID 36791369 – SOD1. (D) RMSD of compound CID 30935 – SOD1. (E) RMSF of SOD1. (F) Interaction profile of the contact between compound CID 30935 – SOD1.
Abbreviations: RMSD: Root-mean-square deviation; RMSF: Root-mean-square fluctuation; SOD1: Superoxide dismutase 1.

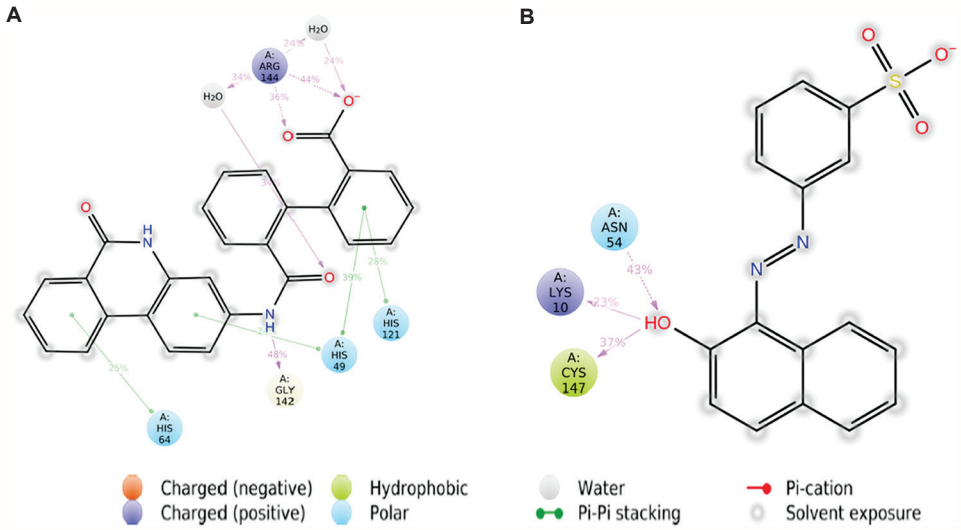

Figure 5. A schematic of detailed ligand-protein interactions. (A) SOD1 with compound CID 36791369. (B) SOD1 with compound CID 30935.
Abbreviation: SOD1: Superoxide dismutase 1.

Table 3. Prime MMGBSA binding energy of interaction of SOD1 with compound CID 36791369 and compound CID 30935, respectively, before and after molecular dynamics simulation

Complex	Simulation time (ns)	MMGBSA ΔG^{bind} (kcal·mol^{-1})							
		Coulomb	Covalent	Hbond	Lipo	Packing	Solv_GB	vdW	G^{bind} (Total)
CID 36791369 – SOD1	0	26.424	8.668	−0.000	−17.151	−5.576	−18.209	−27.025	−32.867
	100	13.001	2.805	−0.611	−15.064	−8.597	−1.900	−45.746	−56.110
CID 30935 – SOD1	0	−3.166	0.816	−1.223	−6.874	−1.900	12.937	−29.108	−28.518
	100	−4.042	4.773	−1.955	−11.130	−1.686	13.991	−39.742	−39.790

Notes: Coulomb: Coulomb energy; Covalent: Covalent binding energy; Hbond: Hydrogen bonding energy; Lipo: Lipophilic energy; Packing: Pi-pi packing correction; Solv GB: Generalized Born electrostatic solvation energy; vdW: van der Waals energy; Total: Total energy (Prime energy).

that both complexes were stable and energetically favorable under simulated physiological conditions.

4. Discussion

SOD1 serves as a therapeutic target for cancer treatment, as inhibiting its activity leads to the downregulation of multiple signaling pathways crucial for endothelial and tumor cell function.[2] PPI analysis of SOD1 in this study revealed its association with other antioxidant genes, the dysfunction or deregulation of which have been implicated in various cancers (e.g., breast cancer and chronic lymphatic leukemia) and neurodegenerative diseases (e.g., ALS and Parkinson's).[27-31]

SOD1 is centrally connected to other proteins encoded by disease-associated genes, which often become prominent components of ubiquitin-positive inclusions found in carriers of corresponding mutations. These proteins include TDP-43, fused in sarcoma, optineurin, ubiquilin-2, ataxin-2, and C9ORF72 (encoded by *TARDBP*, *FUS*, *OPTN*, *UBQLN*, *ATXN2*, and *C9ORF72* genes, respectively).[31,32]

A potential mechanism underlying SOD1 pathogenesis in ALS involves gain-of-interaction, where mis-folded soluble SOD1 forms abnormal PPIs with various cellular proteins, including other SOD1 molecules, thereby disrupting their function. These aberrant PPIs are associated with numerous human diseases, such as cancer, infectious diseases, and neurodegenerative disorders.[33] Identifying and studying PPI networks in disease states is crucial for developing therapies targeting interactions that play functional roles in disease progression and patient outcomes.[34]

Compound SN1 (PubChem CID: 36791369), with the IUPAC name 2-[2-[(6-oxo-5H-phenanthridin-3-yl) carbamoyl]phenyl]benzoate, is a patented compound known to differentially modulate connexin and/or pannexin hemichannels in astrocytes without affecting gap junctions. It finds applications in the treatment of psychiatric disorders.[35] Inhibition of SOD1 protects protein tyrosine phosphatases from oxidation by preventing the formation of hydrogen peroxide, thereby inhibiting ERK phosphorylation in cells stimulated with EGF, FGF-2, or IGF-1.[2] The activity of growth factors such as EGF, IGF-1, PDGF, and VEGF is redox-regulated. When a growth factor binds to its receptor tyrosine kinase, it activates the production of reactive oxygen species, leading to phosphatase inactivation and favoring phosphorylation within cells, thus allowing kinase cascades to propagate.[2] In addition, inhibition of SOD1 by tetrathiomolybdate increases the steady-state levels of superoxide in human umbilical vein endothelial cells, inhibiting their proliferation and subsequently abolishing FGF-2- and VEGF-mediated ERK1/2 phosphorylation.[36]

The compounds obtained in this study were mostly not BBB permeants and not P-gp substrates, exhibited good solubility, and only a few exhibited inhibitory effects on selected cytochrome P450s (CYP2C9, CYP2C19, CYP3A4, CYP1A2, and CYP2D6). This result suggests that their bioavailability is affected by CYPs through the first-pass effect rather than P-gp. Specifically, compounds SN5, SN6, SN7, SN12, and SN25 exhibited BBB permeant features and had moderate to no inhibitory effects on CYPs. P-gp can influence drug bioavailability, and its modulation is considered in drug development to enhance efficacy.[37] Modulation of CYP activities can alter drug metabolism profiles, affecting bioavailability or efficacy.[38]

In this study, compounds SN1, SN5, SN6, SN7, SN12, SN19, SN20, SN25, and SN36 exhibited sufficient binding affinity, with values less than -5.0 kcal·mol^{-1}. Previous research has identified specific SOD1 amino acid residues involved in hydrogen bond formation with various compounds, including L-methionine, aniline (2-methoxy-5-methylaninline), and 2-trifluoromethyl-4-aminoquinazoline.[39] Notably, compounds SN5, SN6, SN7, and SN25 in this study were quinazoline-based compounds. Another study proposed SOD1 as a target of the LCS-1 compound, with the IUPAC name 4,5-dichloro-2-m-tolylpyridazin-3(2H)-one.[13]

Disrupting SOD1 activity has been shown to inhibit cell growth and enhance lipid accumulation in nasopharyngeal carcinoma, a commonly occurring cancer with the highest incidence of malignant proliferation among head and neck cancers.[40] SOD1 mRNA has been reported to be significantly increased in head and neck cancer tissues, according to data from the Oncomine microarray database (https://www.oncomine.org). Multiple signaling pathways, including ERK, NF-κB, and PI3K-Akt, which are essential for the onset and development of cancer, can be activated by intracellularly sustained high levels of hydrogen peroxide provided by elevated activity and expression of copper/zink-containing SOD1. The use of SOD1 inhibitors, including LD100, U0126, LY294002, and BAY117082, has been reported to attenuate some of these signaling pathways.[41]

Molecular docking was utilized to assess the binding affinity of the protein with the ligand, facilitating the determination of the binding site and type of inhibitions. A binding affinity score of ≤ -5.00 kcal·mol^{-1} indicates a good ligand-protein interaction.[42] A previous computational study utilizing molecular docking and MDS has demonstrated that 2,3,5,4'-tetrahydroxystilbene-2-O-β-D-glucoside, hesperidin, and hyperoside have high affinity to mutant SOD1, which is relevant to ALS.[43]

MDSs were then conducted to evaluate atomic-level variations in the protein-ligand system and assess the stability of the protein-ligand complex in a dynamic environment.[44] RMSD values less than 4 Å suggest relatively small conformational changes in the complexes during the simulation, indicating their stability.[45] In addition, the RMSF is useful for characterizing local changes along the protein chain. Prime MMGBSA provided various energy properties, reporting energies for the ligand, receptor, and complex structures, as well as energy differences related to strain and binding.[26] The more negative the score, the higher the free energy released in complex formation. The total binding free energy confirmed the stability of the complexes under physiological conditions, indicating their reasonable stability. A high total energy indicates a strong binding affinity between the molecules. However, the interpretation depends on the specific contributions of individual energy terms and the context of the study.

In this study, the MMGBSA binding energy of the compound CID 30935 – SOD1 complex is influenced by several contributing energies, such as Coulomb, covalent, and hydrogen bonding. A high Coulomb energy indicates robust electrostatic interactions between charged groups, suggesting either strong attraction or repulsion between the binding partners. Understanding these interactions is significant for elucidating the stability or specificity of the binding interaction. Meanwhile, a high covalent binding energy suggests the formation of strong covalent bonds between the binding partners, which may indicate a stable binding complex. However, it is important to note that in drug design, covalent binding can sometimes lead to undesirable side effects, necessitating careful consideration. Moreover, a high hydrogen-bonding correction suggests the formation of strong hydrogen bonds between the binding partners, contributing to the specificity and stability of the binding interaction.

Regarding the compound CID 36791369 – SOD1 complex, MMGBSA binding energy relies on various contributory energies, such as lipophilic, pi-pi, generalized Born electrostatic solvation, and van der Waals interactions. High lipophilic energy suggests robust hydrophobic interactions, which are important for stabilizing binding complexes, especially within hydrophobic pockets of proteins. However, excessively high lipophilic energy might indicate a propensity for non-specific binding to hydrophobic regions. Similarly, high pi-pi packing correction indicates strong interactions between aromatic rings, which are essential for stabilizing binding complexes, especially in protein-ligand interactions. Moreover, high solvation energy may suggest strong interactions between the solute and solvent molecules, potentially affecting the overall stability of the binding complex. However, excessively high solvation energy could imply poor solubility or unfavorable interactions with the solvent. High van der Waals energy indicates robust, attractive interactions between non-polar groups, contributing to the stability of the binding complex. However, excessively high van der Waals energy might lead to non-specific binding or aggregation.

5. Conclusion

This study explored several inhibitors of human SOD1 using enrichment virtual screening, docking, ADME prediction, and molecular dynamics simulation. Among the 42 compounds selected for thorough analyses, five demonstrated favorable ADME properties, promoting BBB permeability and high GIA. In addition, seven compounds exhibited binding affinity values of less than -5.00 kcal·mol^{-1} for SOD1, indicating robust interaction. Specifically, compounds SN5, SN6, SN7, SN12, and SN25 emerged as potential SOD1inhibitors. Further research will be necessary to investigate the therapeutic effectiveness of these top five compounds in both *in vitro* and *in vivo* settings against SOD1.

Acknowledgments

None.

Funding

None.

Conflict of interest

No conflicts of interest to declare.

Author contributions

Conceptualization: Ayodele Sunday Alonge, Toluwase Hezekiah Fatoki, Iseoluwa Isaac Ajayi

Format analysis: Ayodele Sunday Alonge, Toluwase Hezekiah Fatoki, Iseoluwa Isaac Ajayi, Courage Dele Famusiwa, Oluwafijimi Adetuyi

Investigation: Ayodele Sunday Alonge, Toluwase Hezekiah Fatoki, Iseoluwa Isaac Ajayi, Ibrahim Olabayode Saliu, Stanley Chukwuejim, Ohunene Esther Joseph

Methodology: Toluwase Hezekiah Fatoki, Ibrahim Olabayode Saliu

Writing – original draft: Ayodele Sunday Alonge, Toluwase Hezekiah Fatoki, Iseoluwa Isaac Ajayi, Courage Dele Famusiwa, Ohunene Esther Joseph

Writing – review & drafting: Ayodele Sunday Alonge, Toluwase Hezekiah Fatoki, Stanley Chukwuejim, Oluwafijimi Adetuyi

Ethics approval and consent to participate

Not applicable.

Consent for publication

Not applicable.

Availability of data

Data used in this study are available on request from the corresponding author.

References

1. Fridovich I. Superoxide radical and superoxide dismutases. *Annu Rev Biochem*. 1995;64:97-112.

   doi: 10.1146/annurev.bi.64.070195.000525

2. Juarez JC, Manuia M, Burnett ME, *et al.* Superoxide dismutase 1 (SOD1) is essential for H_2O_2-mediated oxidation and inactivation of phosphatases in growth factor signaling. *Proc Natl Acad Sci U S A*. 2008;105(20):7147-7152.

   doi: 10.1073/pnas.0709451105

3. Ticozzi N, Tiloca C, Morelli C, *et al.* Genetics of familial amyotrophic lateral sclerosis. *Arch Ital Biol*. 2011;149(1):65-82.

   doi: 10.4449/aib.v149i1.1262

4. Andersen PM, Al-Chalabi A. Clinical genetics of amyotrophic lateral sclerosis: What do we really know? *Nat Rev Neurol*. 2011;7(11):603-615.

   doi: 10.1038/nrneurol.2011.150

5. Rosen DR, Siddique T, Patterson D, *et al.* Mutations in Cu/Zn superoxide dismutase gene are associated with familial amyotrophic lateral sclerosis. *Nature*. 1993;362(6415):59-62.

   doi: 10.1038/362059a0

6. Sibilla C, Bertolotti A. Prion properties of SOD1 in amyotrophic lateral sclerosis and potential therapy. *Cold Spring Harbor Perspect Biol*. 2017;9(10):a024141.

   doi: 10.1101/cshperspect.a024141

7. Ligon LA, LaMonte BH, Wallace KE, Weber N, Kalb RG, Holzbaur EL. Mutant superoxide dismutase disrupts cytoplasmic dynein in motor neurons. *Neuroreport*. 2005;16(6):533-536.

   doi: 10.1097/00001756-200504250-00002

8. Zhang F, Strom AL, Fukada K, Lee S, Hayward LJ, Zhu H. Interaction between familial amyotrophic lateral sclerosis (ALS)-linked SOD1 mutants and the dynein complex. *J Biol Chem*. 2007;282(22):16691-16699.

   doi: 10.1074/jbc.M609743200

9. Elchuri S, Oberley TD, Qi W, *et al.* CuZnSOD deficiency leads to persistent and widespread oxidative damage and hepatocarcinogenesis later in life. *Oncogene*. 2005;24(3):367-380.

   doi: 10.1038/sj.onc.1208207

10. Busuttil RA, Garcia AM, Cabrera C, *et al*. Organ-specific increase in mutation accumulation and apoptosis rate in CuZn-superoxide dismutase-deficient mice. *Cancer Res*. 2005;65(24):11271-11275.

    doi: 10.1158/0008-5472.CAN-05-2980

11. Ho YS, Gargano M, Cao J, Bronson RT, Heimler I, Hutz RJ. Reduced fertility in female mice lacking copper-zinc superoxide dismutase. *J Biol Chem*. 1998;273(13):7765-7769.

    doi: 10.1074/jbc.273.13.7765

12. Blander G, De Oliveira RM, Conboy CM, Haigis M, Guarente L. Superoxide dismutase 1 knock-down induces senescence in human fibroblasts. *J Biol Chem*. 2003;278(40):38966-38969.

    doi: 10.1074/jbc.M307146200

13. Somwar R, Erdjument-Bromage H, Larsson E, *et al.* Superoxide dismutase 1 (SOD1) is a target for a small molecule identified in a screen for inhibitors of the growth of lung adenocarcinoma cell lines. *Proc Natl Acad Sci U S A*. 2011;108(39):16375-16380.

    doi: 10.1073/pnas.1113554108

14. Szklarczyk D, Gable AL, Nastou KC, *et al.* The STRING database in 2021: Customizable protein-protein networks, and functional characterization of user-uploaded gene/measurement sets. *Nucleic Acids Res*. 2021;49(D1):D605-D612.

doi: 10.1093/nar/gkaa1074

15. Backman TW, Cao Y, Girke T. ChemMine tools: An online service for analyzing and clustering small molecules. *Nucleic Acids Res*. 2011;39:W486-W491.

doi: 10.1093/nar/gkr320

16. Daina A, Michielin O, Zoete V. SwissADME: A free web tool to evaluate pharmacokinetics, drug-likeness and medicinal chemistry friendliness of small molecules. *Sci Rep*. 2017;7:42717.

doi: 10.1038/srep42717

17. Fatoki T, Chukwuejim S, Ibraheem O, *et al.* Harmine and 7,8-dihydroxyflavone synergistically suitable for amyotrophic lateral sclerosis management: An *in silico* study. *Res Results Pharmacol*. 2022;8(3):49-61.

doi: 10.3897/rrpharmacology.8.83332

18. Morris GM, Huey R, Lindstrom W, *et al.* AutoDock4 and AutoDockTools4: Automated docking with selective receptor flexibility. *J Comput Chem*. 2009;30(16):2785-2791.

doi: 10.1002/jcc.21256

19. Trott O, Olson AJ. AutoDock Vina: Improving the speed and accuracy of docking with a new scoring function, efficient optimization, and multithreading. *J Comput Chem*. 2010;31(2):455-461.

doi: 10.1002/jcc.21334

20. Eberhardt J, Santos-Martins D, Tillack AF, Forli S. AutoDock vina 1.2.0: New docking methods, expanded force field, and python bindings. *J Chem Inf Model*. 2021;61(8):3891-3898.

doi: 10.1021/acs.jcim.1c00203

21. Tao A, Huang Y, Shinohara Y, Caylor ML, Pashikanti S, Xu D. ezCADD: A rapid 2D/3D visualization-enabled web modeling environment for democratizing computer-aided drug design. *J Chem Inf Model*. 2019;59(1):18-24.

doi: 10.1021/acs.jcim.8b00633

22. Schrödinger. *Schrödinger Release 2018-3. Desmond Molecular Dynamics Syste*m. New York: D.E. Shaw Research, Maestro Desmond Interoperability Tools, Schrödinger; 2018.

23. Ali I, Iqbal MN, Ibrahim M, Haq IU, Alonazi WB, Siddiqi AR. Computational exploration of novel ROCK2 inhibitors for cardiovascular disease management; insights from high-throughput virtual screening, molecular docking, DFT and MD simulation. *PLoS One*. 2023;18(11):e0294511.

doi: 10.1371/journal.pone.0294511

24. Fatoki TH, Faleye BC, Nwagwe OR, *et al*. Friedelin could moderately modulate human carbonic anhydrases: An *in silico* study. *Bioint Res Appl Chem*. 2024;14(2):49.

doi: 10.33263/BRIAC142.049

25. Fatoki TH. Effect of pH on structural dynamics of HMG-CoA reductase and binding affinity to β-sitosterol. *J Biomol Struct Dyn*. 2023;41(10):4398-4404.

doi: 10.1080/07391102.2022.2067240

26. Schrödinger. *What do All the Prime MM-GBSA Energy Properties Mean*? 2019. Available from: https://www.schrodinger.com/kb/1875 [Last accessed on 2023 Nov 20].

27. Richarme G, Mihoub M, Dairou J, Bui LC, Leger T, Lamouri A. Parkinsonism-associated protein DJ-1/Park7 is a major protein deglycase that repairs methylglyoxal- and glyoxal-glycated cysteine, arginine, and lysine residues. *J Biol Chem*. 2015;290(3):1885-1897.

doi: 10.1074/jbc.M114.597815

28. Perini GF, Ribeiro GN, Pinto Neto JV, Campos LT, Hamerschlak N. BCL-2 as therapeutic target for hematological malignancies. *J Hematol Oncol*. 2018;11(1):65.

doi: 10.1186/s13045-018-0608-2

29. Sugiyama T, Murao N, Kadowaki H, *et al.* ERAD components Derlin-1 and Derlin-2 are essential for postnatal brain development and motor function. *iScience*. 2021;24(7):102758.

doi: 10.1016/j.isci.2021.102758

30. Olivo E, La Chimia M, Ceramella J, *et al.* Moving beyond the Tip of the Iceberg: DJ-1 implications in cancer metabolism. *Cells*. 2022;11(9):1432.

doi: 10.3390/cells11091432

31. Fatoki TH, Chukwuejim S, Udenigwe CC, Aluko RE. *In silico* exploration of metabolically active peptides as potential therapeutic agents against amyotrophic lateral sclerosis. *Int J Mol Sci*. 2023;24(6):5828.

doi: 10.3390/ijms24065828

32. Blokhuis AM, Groen EJ, Koppers M, Van den Berg LH, Pasterkamp RJ. Protein aggregation in amyotrophic lateral sclerosis. *Acta Neuropathol*. 2013;125(6):777-794.

doi: 10.1007/s00401-013-1125-6

33. Lu H, Zhou Q, He J, *et al.* Recent advances in the development of protein-protein interactions modulators: Mechanisms and clinical trials. *Signal Transd Targeted Ther*. 2020;5:213.

doi: 10.1038/s41392-020-00315-3

34. Kuzmanov U, Emili A. Protein-protein interaction networks: Probing disease mechanisms using model systems. *Genome Med*. 2013;5(4):37.

doi: 10.1186/gm441

35. National Center for Biotechnology Information. PubChem Patent Summary for US-2015337018-A1. Available from: https://pubchem.ncbi.nlm.nih.gov/patent/US-2015337018-A1 [Last accessed on 2023 Dec 04].

36. Juarez JC, Betancourt O Jr., Pirie-Shepherd SR, *et al.* Copper binding by tetrathiomolybdate attenuates angiogenesis and tumor cell proliferation through the inhibition of superoxide

dismutase 1. *Clin Cancer Res*. 2006;12(16):4974-4982.

doi: 10.1158/1078-0432.CCR-06-0171

37. Fatoki TH, Awofisayo OA, Ibraheem O, Oyedele AS, Akinlolu OS. *In silico* investigation of first-pass effect on selected small molecule excipients and structural dynamics of P-glycoprotein. *Bioinform Biol Insights*. 2020;14:1177932220943183.

doi: 10.1177/11779322209431

38. Martin P, Giardiello M, McDonald TO, Rannard SP, Owen A. Mediation of *in vitro* cytochrome P450 activity by common pharmaceutical excipients. *Mol Pharm*. 2013;10:2739-2748.

doi: 10.1021/mp400175n

39. Antonyuk S, Strange RW, Hasnain SS. Structural discovery of small molecule binding sites in Cu-Zn human superoxide dismutase familial amyotrophic lateral sclerosis mutants provides insights for lead optimization. *J Med Chem*. 2010;53(3):1402-1406.

doi: 10.1021/jm9017948

40. Li S, Fu L, Tian T, *et al.* Disrupting SOD1 activity inhibits cell growth and enhances lipid accumulation in nasopharyngeal carcinoma. *Cell Commun Signal*. 2018;16:28.

doi: 10.1186/s12964-018-0240-3

41. Li X, Chen Y, Zhao J, *et al*. The specific inhibition of SOD1 selectively promotes apoptosis of cancer cells via regulation of the ROS signaling network. *Oxid Med Cell Longev*. 2019;2019:9706792.

doi: 10.1155/2019/9706792

42. Wong F, Krishnan A, Zheng EJ, *et al.* Benchmarking AlphaFold-enabled molecular docking predictions for antibiotic discovery. *Mol Syst Biol*. 2022;18(9):e11081.

doi: 10.15252/msb.202211081

43. Huang HJ, Chang TT, Chen HY, Chen CY. Finding inhibitors of mutant superoxide dismutase-1 for amyotrophic lateral sclerosis therapy from traditional Chinese medicine. *Evid Based Complement Alternat Med*. 2014;2014:156276.

doi: 10.1155/2014/156276

44. Fatoki TH. Human adenovirus DNA polymerase is evolutionarily and functionally associated with human telomerase reverse transcriptase based on *in silico* molecular characterization that implicate abacavir and zidovudine. *Front Bioinform*. 2023;3:1123307.

doi: 10.3389/fbinf.2023.1123307

45. Fatoki TH, Balogun CT, Oluwadare OT, *et al. In silico* evaluation of nutri-pharmacological potentials of phytochemicals in sorghum (*Sorghum* bicolor) grains. *J Food Bioact*. 2023;23:18354.

doi: 10.31665/JFB.2023.18354